# Epitaxial Growth, Processing and Characterization of Semiconductor Nanostructures

Borgström, Magnus

2003

Available online at www.sciencedirect.com
SCIENCE DIRECT®
Journal of Crystal Growth 252 (2003) 481–485
JOURNAL OF CRYSTAL GROWTH
www.elsevier.com/locate/jcrysgro

# InAs quantum dots grown on InAlGaAs lattice matched to InP

M. Borgstrom[a,b,*], M.P. Pires[a], T. Bryllert[b], S. Landi[a], W. Seifert[b], P.L. Souza[a]

[a] *Laboratório de Semicondutores-Centro de Estudos em Telecomunicações, Pontifica Universidade Católica do Rio de Janeiro, Rua Marqués de São Vicente 225, 22453 Rio de Janeiro, Brazil*
[b] *Department of Solid State Physics, University of Lund, Box 118, S-221 00 Lund, Sweden*

Received 9 November 2002; accepted 16 January 2003
Communicated by J.B. Mullin

**Abstract**

In this paper, we present InAs quantum dots prepared on an $In_xAl_yGa_{1-x-y}As$ surface by metal organic vapor phase epitaxy. Atomic force microscopy measurements indicate that dots grown on material with higher Al content are smaller, and that the local dot densities on step-bunched facets formed on the vicinal (0 0 1) surfaces increase. We find that these dots show luminescence at very long wavelengths, $\lambda_{\text{room temperature}} \approx 2.1\,\mu m$, and that the emission wavelengths are blue-shifted when the Al content is increased in the layer onto which dot material is deposited.


*PACS:* 68.55.Jk; 71.55.Eq; 81.15.Gh

*Keywords:* A1. Nanostructures; A3. Metalorganic vapor phase epitaxy; B2. Semiconducting III–V materials

## 1. Introduction

The self-assembled formation of three-dimensional islands is considered to be one of the most promising ways to make defect-free quantum dots (QDs). QD lasers have been extensively studied due to predicted low threshold current operation [1,2], low chirp [3] and temperature insensitive operation [4], due to the delta function-like density of states of the dots. The recent experimental realization of QD lasers confirming low threshold current density [5], low chirp [6] and temperature insensitive operation has sparked that interest. For a review of QD lasers, see Ref. [7].

Typical QD semiconductor lasers, fabricated with InAs QDs on GaAs substrate, operate at wavelengths as long as 1.2 μm, with longer wavelengths achievable by the use of InGaAs capped InAs dots [8]. There is great interest in being able to extend this wavelength to 1.55 μm, and beyond, for use in fiber optic telecommunication systems. Growth of InAs QDs on InP allows for these wavelengths to be readily reached [9–11]. Lasing from InAs QDs grown on GaInAs lattice matched to InP has been reported [12–14], which lased at a wavelength of 1.9 μm.

For laser applications, it is desirable to achieve samples with a high density of QDs in a narrow

*Corresponding author. Department of Solid State Physics, University of Lund, Box 118, S-221 00 Lund, Sweden. Tel.: +46-2227671; fax: +46-2223637.
*E-mail address:* magnus.borgstrom@ftf.lth.se (M. Borgstrom).

0022-0248/03/$ - see front matter 
doi:10.1016/S0022-0248(03)00969-2

size distribution, without degrading the optical efficiency. Furthermore, it would be advantageous to have a large refractive index change between the active region and the surrounding InP. For improved temperature characteristics one can qualitatively conclude that the discrete quantum levels should be widely separated in energy and confined by a deep potential well to isolate the ground state from the wetting layer. The use of pure InGaAs as barrier material is expected to give a small electron confinement and a poor high-temperature performance, whereas a barrier material of pure InAlAs would result in a lower change in the refractive index with respect to InP. Therefore $In_xAl_yGa_{1-x-y}As$ is preferred as barrier material, as compared to the ternaries.

For this purpose, we have grown InAs QDs on $In_xAl_yGa_{1-x-y}As$, lattice matched to InP, in low-pressure (50 mbar) metal organic vapor phase epitaxy (MOVPE). We studied the effect of varying the Al content in the quaternary compound from 0% to 23% on dot formation. The tunability of the room temperature bandgap $E_g$ of $In_xAl_yGa_{1-x-y}As$ is given by $0.75 < E_g < 1.46\,eV$ where the refractive index $n_i$ of the compound is given by $3.41 < n_i < 3.22$; the values for pure InGaAs are to the left and the values for pure InAlAs are to the right and for pure InP $n_{InP} = 3.10$.

## 2. Experimental procedure

The samples were grown by MOVPE with phosphine ($PH_3$), arsine ($AsH_3$), trimethyl-indium (TMI), trimethyl-gallium (TMG), and trimethyl-aluminium (TMA) as precursors, and hydrogen as carrier gas. The process was controlled by a flow and pressure balanced ventilation/run system. The total gas flow in the reactor cell was about 6000 $cm^3$/min. We used Fe-doped (SI) InP (0 0 1) "epi-ready" wafers with a 2° misorientation towards the nearest ⟨0 1 1⟩ direction for our experiments. A 150 nm thick InP buffer layer was grown, initially at an elevated growth temperature of 630°C, after which the reactor was cooled down to 600°C. Then a 500 nm thick $In_xAl_yGa_{1-x-y}As$ layer was grown with a V/III ratio of 30. The growth rates for InP and $In_xAl_yGa_{1-x-y}As$ were 1.4 and 2.8 ML/s, respectively. The temperature was ramped down to 500°C during a 5 min period without growth, to keep the well-defined terrace structure before dot deposition. 2.5 ML InAs dot material was deposited on the surface at a growth rate of 0.5 ML/s and then the surface was annealed for 12 s under an arsine flow. At this point, the samples were either cooled down under arsine containing atmosphere, or capped with 50 nm InP during which the temperature was ramped up to 600°C. For capping the samples, the arsine was switched off and replaced by phosphine. Then TMI was reintroduced into the reactor, after a delay time of 1 s in order to reduce carry over effects [15].

Photoluminescence (PL) of capped dot structures was measured by Fourier transform infrared spectroscopy with the samples either immersed in liquid nitrogen, or in air at room temperature. As excitation source we used an Ar-ion laser with an excitation power of 50 mW. An InSb detector was used for detection.

For non-capped samples, the lattice matching of the quaternary layer was checked by a combination of PL and X-ray diffraction measurements. The Al content in the $In_xAl_yGa_{1-x-y}As$ layers, lattice matched to InP, was varied between 0% and 23%. Surfaces were then studied with tapping-mode atomic force microscopy (AFM). The height distributions of the islands were evaluated by measuring the height of 324 islands from respective AFM image, and from these data histograms were made. We take the height values as representative for the size of the islands. The dot densities were evaluated by counting the islands on $2 \times 2\,\mu m^2$ images.

## 3. Results and discussion

Initially the effect on dot formation when Al is introduced into the layer onto which dot material is deposited was studied. Fig. 1a–c shows AFM images and corresponding height histograms of InAs QDs on $In_xAl_yGa_{1-x-y}As$, with increasing Al content from (a) to (c). After the critical wetting layer thickness is reached and after a nucleation

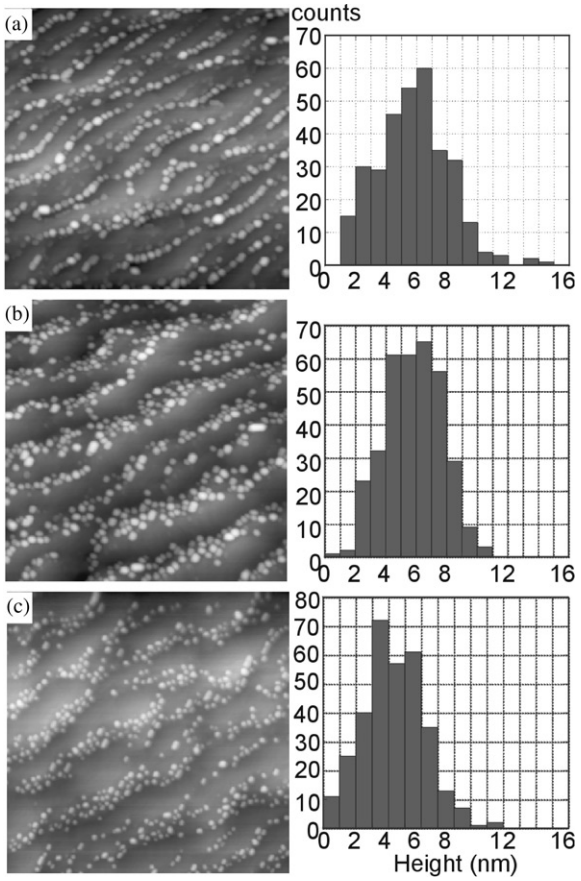


Fig. 1. $2 \times 2\,\mu m^2$ AFM images with corresponding height histograms taken after 2.5 ML InAs deposition on $In_xAl_y$-$Ga_{1-x-y}As$ with (a) $y = 0$, (b) $y = 0.11$, (c) $y = 0.16$.

process, dots form by consuming material from the wetting layer as well as from the continuous deposition of material. InAs species diffuse on the surface over the remaining InAs wetting layer, which to some degree contains Al and Ga due to intermixing. We observe stronger step bunching on the vicinal substrates for dots grown on Al containing layers. This agrees with previous modeling by Liu et al. They showed that step bunching should increase with smaller diffusion constant for a species on vicinal surfaces [16]. The reduced diffusion length is thought to arise from the increased bond strength of the intermixed Al containing material in the wetting layer. This can slow down column III atom migration on the crystal surface, in agreement with previously reported results of InGaAlAs QDs on GaAs [17]. There was no obvious quantitative dependence on the amount of Al used, although its presence was significant. The homogeneity of the QDs increases, which also can be seen in Table 1. As seen from the height histograms, the mean dot heights decrease with higher Al contents.

Fig. 2 shows the alignment of dots along the multi steps. The dots first nucleate at the intersection between the step-bunched facet and the lower vicinal (0 0 1) terrace (Fig. 2a). This is similar to previous observations by Kitamura et al. [18]. On our samples with increasing Al content, the

Table 1
Data derived from AFM images and PL measurements from samples with varied Al content (for abbreviations see text).

| % | $\rho$ ($cm^{-2}$) | height (nm) | SD | FWHM (meV) | $\lambda$ (μm) | $E$ (eV) |
|---|---|---|---|---|---|---|
| 0 | 1.5 | 5.7 | 2.41 | 65 | 2.10 | 0.59 |
| 6 | 1.5 | 5.8 | 1.99 | 72 | 2.03 | 0.61 |
| 11 | 1.2 | 6.1 | 2.35 | 71 | 2.00 | 0.62 |
| 16 | 1.5 | 5.2 | 1.86 | 77 | 2.01 | 0.62 |
| 23 | 2.5 | 4.3 | 1.38 | 77 | 1.99 | 0.63 |

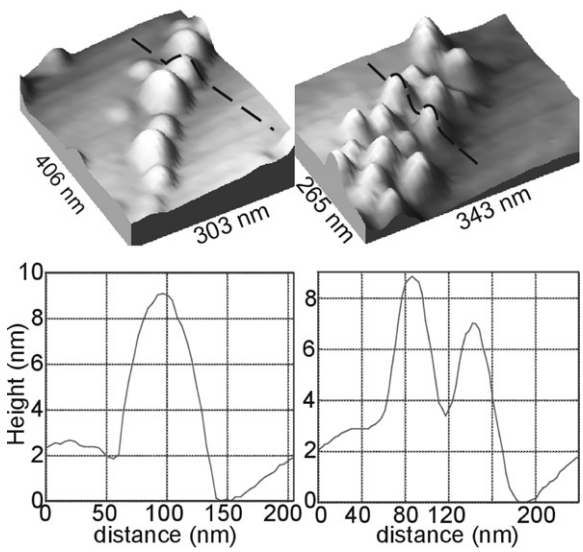


Fig. 2. 3D AFM images of dots at step-bunches on (a) GaInAs (b) $In_{0.52}Al_{0.16}Ga_{0.32}As$ and corresponding surface line-scans. Line scans are indicated in (a) and (b).

bunching gets stronger and the local density of dots at the step bunch becomes higher, and the dot sizes become smaller. Dots now cover the entire step bunched facet (Fig. 2b). Due to AFM convolution effects it is difficult to determine the correct dot widths. However, it can clearly be seen that for the pure GaInAs, the dot is larger, extending over 80 nm in apparent width, whereas for the 16% Al sample, two dots nucleate at the step bunch, their base widths extending over 110 nm in total. Therefore the dots seem to be similar, only the size has changed. We expected the total dot density to increase with the addition of Al, however for small amounts of Al this is not true. We speculate that this non-consistency can be explained if, due to the introduction of Al and thereby the increased bond strength, the critical wetting layer thickness for dot formation increases. As a consequence, less material of the wetting layer would be available for dot formation.

Fig. 3 shows the PL from InAs QDs on $In_xAl_yGa_{1-x-y}As$ with different Al content at room temperature. With increasing Al content, the emission energy of the dots increases for two reasons: Firstly, the higher density of dots (using the same amount of dot material) leads to a smaller dot size, due to materials distribution over the nuclei, and thereby to an increased quantum confinement of the dot. Secondly, the larger the Al content in the barrier material, the larger its bandgap. Both effects influence the electronic level structure of the dots. Thus, the emission wavelength of the dots can, in principle, be tuned by adjusting the Al content in the barrier material. For QDs on the pure GaInAs, a wetting layer peak can be observed at 0.72 eV. The wetting layer peak disappears when we introduce Al into the quaternary compound, indicating that the carrier capture from wetting layer to dots is then more effective. This, we believe, is due to the increased potential barrier that results in more highly confined, but also deeper electron states within the dots (with consideration to the surrounding barrier), which therefore suppresses thermally activated escape of carriers from the dots to the wetting layer or GaInAs. The separation in energy between the ground state in the dots and the wetting layer states increases, with increasing Al,

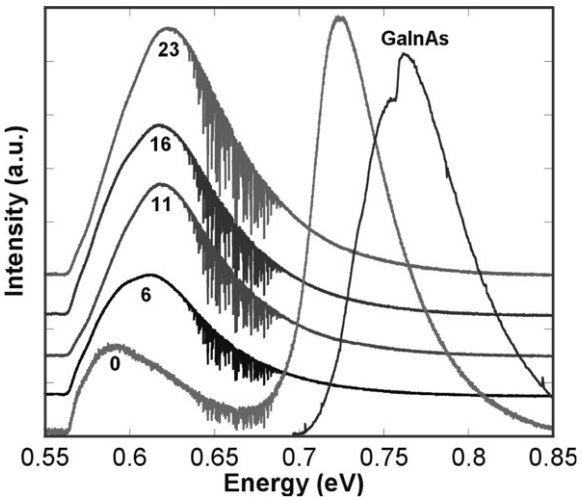


Fig. 3. Room temperature PL from InAs QDs on $In_xAl_y$-$Ga_{1-x-y}As$, capped with InP, the numbers indicate the Al content ($x$%). The peaks are offset for clarity. The peak measured from bulk GaInAs is also shown.

causing a stronger driving force for drift of carriers into the dots. This wetting layer peak is not seen in data taken at 77 K. The PL observed from pure GaInAs bulk material is also presented, with its peak at 0.76 eV. The peaks, originating in luminescence from the dots, are observed between 0.59 eV up to 0.63 eV, which corresponds to the very long wavelengths of up to 2.1 μm. The dots were capped by InP. This affects the dot emission compared with the structure where they were capped by $In_xAl_yGa_{1-x-y}As$ with the same materials composition that they were deposited on. The InP bandgap is larger and As/P exchange reactions occur when InP caps the dots. We used InP in order to make a comparison between AFM and PL data, being able to rule out complicated phase separation effects [19]. In the PL spectra, what seems to be noise at around 0.67 eV, is water absorption that occurs as the emission passes through air before entering the spectrometer. In Table 1, a collection of the data obtained by AFM and PL measurements are presented. For the AFM measurements, a Gaussian size distribution was assumed, and simulated to fit the obtained height diagrams. SD in Table 1 shows the standard deviation for these fitted curves, and it is a measure of the size homogeneity of the dots. The results

indicate that the dots become more homogeneous with the insertion of Al into the layer immediately beneath the InAs. It is interesting to note that the PL measurements show the opposite trend, something that possibly could be explained by the observed shift in dot size. A narrow apparent dot size only (as observed by AFM), will not correctly reflect the distribution of the electronic states within the dots since a change in dot size for a smaller dot has relatively larger impact on the change in quantization energy.

## 4. Conclusions

In summary, self-assembled InAs quantum dots have been deposited on $In_xAl_yGa_{1-x-y}As$ with varying Al content, lattice matched to InP. Ensembles of coherent dots were formed on the $In_xAl_yGa_{1-x-y}As$ with a shift to smaller dot sizes with increasing Al content. Very long wavelengths of emission of up to 2.1 μm were seen in PL measurements from the dots, with a decreasing wavelength for the higher Al containing samples. Growth temperature, deposition rate, and V/III ratio are adjustable parameters that offer additional possibilities of tuning the electronic states of the dots, and consequently also the energy of light emission in devices based on InAs/$In_xAl_yGa_{1-x-y}As$ quantum dot structures

## Acknowledgements

The authors are grateful to Dr. Rodrigo Prioli for assistance in AFM measurements. The work was supported by Faperj, CNPq, MCT-Instituto do Milênio de Nanociências and MCT-Rede de Nanociências.

## References

[1] M. Asada, A. Kameyama, Y. Suematsu, IEEE J. Quantum Electron. 20 (1984) 745.
[2] Y. Miyamoto, Y. Miake, M. Asada, Y. Suematsu, IEEE J. Quantum Electron. 25 (1989) 2001.
[3] M. Grundmann, J. Christen, N.N. Ledentsov, J. Böhrer, D. Bimberg, S.S. Ruvimov, P. Werner, U. Richter, U. Gösele, J. Heydenreich, V.M. Ustinov, Y. Egorov, A.E. Zhukov, P.S. Kopév, Z.I. Alferov, Phys. Rev. Lett. 74 (1995) 4043.
[4] Y. Arakawa, H. Sakaki, Appl. Phys. Lett. 40 (1982) 939.
[5] N. Kirstaedter, N.N. Ledentsov, M. Grundmann, D. Bimberg, V.M. Ustinov, S.S. Ruvimov, M.M. Maximov, P.S. Kopév, Z.I. Alferov, U. Richter, P. Werner, U. Gösele, J. Heydenreich, Electron. Lett. 30 (1994) 1416.
[6] H. Saito, K. Nishi, A. Kamei, S. Sugou, IEEE Photonics Technol. Lett. 12 (2000) 1298.
[7] M. Grundmann, Physica E 5 (2000) 167.
[8] K. Nishi, H. Saito, S. Sugou, J.-S. Lee, Appl. Phys. Lett. 74 (1999) 1111.
[9] S. Fafard, Z. Wasilewski, J. McCaffrey, S. Raymond, S. Charbonneau, Appl. Phys. Lett. 68 (1995) 991.
[10] N. Carlsson, T. Junno, L. Montelius, M.-E. Pistol, L. Samuelson, W. Seifert, J. Crystal Growth 191 (1998) 347.
[11] P.J. Poole, J. McCaffrey, R.L. Williams, J. Lefebvre, D. Chithrani, J. Vac. Sci. Technol. B 19 (2001) 1467.
[12] V.M. Ustinov, A.R. Kovsh, A.E. Zhukov, A.Y. Egorov, N.N. Ledentsov, A.V. Lunev, Y.M. Shernyakov, M.V. Maksimov, A.F. Tsatsuĺnikov, B.V. Volovik, P.S. Kopév, Z.I. Alferov, Tech. Phys. Lett. 24 (1998) 22.
[13] V.M. Ustinov, A.E. Zhukov, A.Y. Egorov, A.R. Kovsh, S.V. Zaitsev, N.Y. Gordeev, V.I. Kopchatov, N.N. Ledentsov, A.F. Tsatsuĺnikov, B.V. Volovik, P.S. Kopév, Z.I. Alferov, S.S. Ruvimov, Z. Liliental-Weber, D. Bimberg, Electron. Lett. 34 (1998) 670.
[14] A.E. Zhukov, A.Y. Egorov, A.R. Kovsh, V.M. Ustinov, S.V. Zaitsev, N.Y. Gordeev, V.I. Kopchatov, A.V. Lunev, A.F. Tsatsuĺnikov, B.V. Volivik, N.N. Ledentsov, P.S. Kopév, Semiconductors 32 (1998) 795.
[15] W. Seifert, D. Hessman, X. Liu, L. Samuelson, J. Appl. Phys. 75 (1994) 1501.
[16] F. Liu, J. Tersoff, M.G. Lagally, Phys. Rev. Lett. 80 (1998) 1268.
[17] O. Baklenov, D.L. Huffaker, A. Anselm, D.G. Deppe, B.G. Streetman, J. Appl. Phys. 82 (1997) 6362.
[18] M. Kitamura, M. Nishioka, J. Oshinowo, Y. Arakawa, Appl. Phys. Lett. 66 (1995) 3663.
[19] M.V. Maximov, A.F. Tsatsuĺnikov, B.V. Volovik, D.S. Sizov, Y.M. Shernyakov, I.N. Kaiander, A.E. Zhukov, A.R. Kovsh, S.S. Mikhrin, V.M. Ustinov, Z.I. Alferov, R. Heitz, V.A. Shchukin, N.N. Ledentsov, D. Bimberg, Phys. Rev. B 62 (1999) 16671.